ATTENUATION OF SOLITARY WAVE BY PARAMETERIZED FLEXIBLE MANGROVE MODELS

Agnieszka Strusińska-Correia[1], Semeidi Husrin[2] and Hocine Oumeraci[1]

The systematic laboratory investigation on tsunami attenuation by flexible mangrove models was performed in order to improve the knowledge on tsunami-coastal forest interaction. A sophisticated parameterization method, based on structural and bio-mechanical properties of a mature mangrove (*Rhizophora sp*.), was developed for the construction of the mangrove models under assumption of stiff and flexible structure. The forest model examined in the laboratory experiments consisted of the selected flexible mangrove models, arranged in different configurations, which was impacted by a tsunami-like solitary wave of varying height, propagating in different water depths. Based on the envelopes of max. wave height and wave forces induced on single tree models, wave evolution modes were determined to identify the source of wave attenuation. The results indicate the dependence of wave transmission on the observed wave evolution modes and relative forest width: the highest transmission coefficient is attributed to nonbreaking waves (ca. 0.78 and 0.55 for forest width of 0.75 and 3.0 m, respectively), while the lowest transmission coefficient corresponds to wave breaking in front of/in the forest model (ca. 0.5 and 0.3 for forest width of 0.75 and 3.0 m, respectively).

eywords: mangroves; parameterization method; solitary wave; wave attenuation; laboratory experiments

INTRODUCTION

The positive role of coastal vegetation in the preservation of coastal ecosystems and in the prevention of the inland from flooding due to storms and cyclones is undisputed – coastal forests have been employed to enhance stabilization of the coastal zone (particularly dunes), to protect the adjacent fields from salt spray and wind, to support fisheries and to dissipate energy of short-period waves (e.g. Badola and Hussain 2005, Wolanski 2007, Mazda et al. 1997b). The recent tsunami events in 2004 and 2011 have attracted public attention to another aspect of the protective role of a coastal forest, in particularly mangroves, namely tsunami mitigation. In many of post-tsunami field survey reports (e.g. Kathiresan and Rajendran 2005, EJF 2006, Yanagisawa et al. 2009), lower casualties and property losses were claimed due to the presence of a dense mangrove forest. However, a detailed insight into the local tsunami hydrodynamics, local topography-bathymetry features and pre-tsunami forest conditions was very often ignored in these reports, what might have led to overestimation of the performance of mangrove forests during the 2004 Indian Ocean Tsunami.

Definitely, performance of a coastal forest is conditioned by several factors such as vegetation characteristics (vegetation type, age, health state, density, width of the green belt), tsunami parameters (height, period, angle of impact), local morphology and soil properties, and is limited by the magnitude of the tsunami event and the tree resistance to wave impact. Although some vegetation zones were found intact after the recent tsunami events, most of them, particularly those facing directly an open sea, were moderately to heavily damaged by tilting, trunk/branches breakage and uprooting (e.g. Shuto 1987, Latief and Hadi 2006, Yanagisawa et al. 2009).

The influence of the above-mentioned parameters on the effectiveness of a mangrove forest in tsunami mitigation has not been addressed in previous experimental investigations. Particularly the lack of a comprehensive parameterization method for the development of a tree model under consideration of structural and bio-mechanical tree properties is the main disadvantage of these studies, enabling comparison of the experimental results. The geometry of mangrove trees was either idealized by using single cylinders representing tree trunk (and thus neglecting the roots and the canopy) or modeled by means of material of very different properties than the prototype (dimensions, stiffness, etc.). Fig. 1 shows selected mangrove models, examined in previous studies.

The parameterization approach applied to the development of a tree model determines the hydrodynamic performance of the forest model considered and the processes accompanying wave-tree interaction. Inappropriate assumptions on structural and bio-mechanical properties of the tree as well as too strong simplification of tree structure may lead to gaining incorrect experimental data and wrong assessment of the damping characteristics of the forest.

[1] Hydromechanics and Coastal Engineering, Technical University Braunschweig, Beethovenstr. 51a, Braunschweig, Lower Saxony, 38106, Germany
[2] Research Institute of Coastal Resources and Vulnerability, Ministry of Marine and Fisheries Affairs, Padang-Painan Km.16, Padang, West Sumatera, 25245, Indonesia

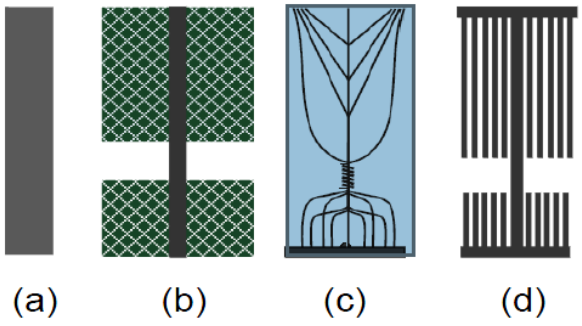

Figure 1. Examples of parameterized mangrove models from previous studies: a) cylinder-shaped model by Massel et al. 1999, b) porous model by Harada and Imamura 2000, c) wire-made model by Istiyanto et al. 2003, d) model by Kongko 2004 with cylinders representing roots, trunk and canopy (after Husrin 2013).

In this paper, the effectiveness of a parameterized mangrove forest in attenuation of a solitary-like tsunami wave is discussed, based on laboratory experiments performed for different forest configurations, water depths and incident wave conditions. The approach proposed for the parameterization of mangrove *Rhizophora sp*., accounting for physical tree properties, represents the core of this study.

DEVELOPMENT OF APPROACH FOR PARAMETERIZATION OF MANGROVES

Considering the wave damping properties of a mangrove in respect to its geometry and bio-mechanical properties, *Rhizophora sp*. with a very dense, wide root system and a well-developed canopy represents mangroves that are most suitable for the purposes of this study (see Fig. 2a). Tree resistance to flow depends largely on tree growth stage, during which tree dimensions, root/canopy density and trunk elasticity change greatly. In order to ensure maximum tree resistance to flow, a mature *Rhizophora sp*. was considered in the parameterization method.

Development of a generic parameterization approach was conditioned by the necessity of use of simple mangrove models in the experiments and the reduction of the effort spent on the preparation of the experimental set-up. Unlike the previous studies, the simplification of mangrove geometry, particularly the complex 3D root system and the canopy, was based on both structural and bio-mechanical properties of a mangrove, under condition of same hydraulic losses in the prototype and the model.

The tree characteristics (i.e. dimensions, trunk elasticity, root and canopy density) was defined using data available from previous studies, extended by own field measurements performed on a young, mid age and mature *Rhizophora apiculata* by Semeidi Husrin in Angke Kapuk Protected Forest Region on Java Island in Indonesia (see Husrin 2013 for more details). When determining a typical geometry of a mature *Rhizophora sp*., shown in Fig. 2b, other available field data by e.g. Mazda et al. 1997a, Istiyanto et al. 2003, Harada and Kawata 2005 were additionally used.

In the literature, values of Young modulus, defining the elasticity of the trunk, range from 8.27×10^9 N/m^2 for 17% of moisture content for *Rhizophora sp*. (Hawa 2005) to 20.03×10^9 N/m^2 for mangroves (Vallam et al. 2011). Young modulus of 13.6×10^9 N/m^2 (for moisture content of ca. 15%) was obtained from deflection tests of wooden probes, performed in the framework of own field surveys.

Concept of a submerged root ratio V_m/V, introduced by Mazda et al. (1997a), was adopted to define the density of the root system as a function of water depth (where V_m represents the volume of submerged roots and V the water control volume). This method required counting of the roots at selected water levels, which in case of the field work by Mazda et al. (1997a) were limited to the tidal level of 0.5 m and were extended up to ca. 1.5 m in own field surveys.

Canopy density was specified using Leaf Area Index (LAI), which represents a ratio of a total one-sided leaves area to the downward projected area of a canopy. By estimating the number of leaves on mangrove main branches, leaves area and number of the branches, LAI of 1.3, 3.3 and 2.9 was determined for a young, mid-age and mature tree, respectively, in own field measurements. In the literature, LAI of ca. 7 was reported for mangroves by Green and Clark (2000), while Clough et al. (2000) underlined its dependency on tree age (LAI > 5.0 for mangroves younger than 5 years, LAI ca. 1.8 for 36 year old mangroves). LAI of 4.5 was considered in this study.

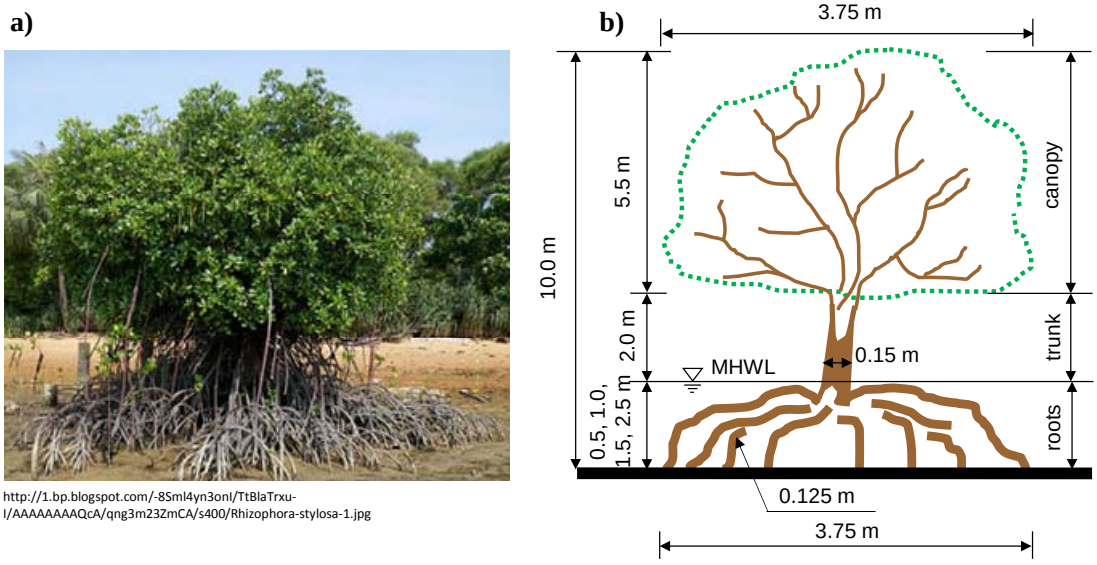

Figure 2. Mature mangrove *Rhizophora sp*. in natural habitat (a) and its geometry (b).

Based on the defined structural and bio-mechanical properties of a mature *Rhizophora sp*., two parameterization approaches were developed in order to determine the contribution of each structural tree element (i.e. the root system, the trunk and the canopy) to wave attenuation, depending on tsunami flow depth:

- Stiff structure assumption, in which the tree model consisted of a parameterized root system and a stiff trunk. The stiff mangrove model was submerged maximally up to the top of the trunk, what corresponded to tsunami of a moderate magnitude (see Strusińska-Correia et al. 2013).
- Flexible structure assumption, in which the tree model consisted of a parameterized root system (identical to the one in the stiff structure assumption), a flexible trunk and a canopy. In this case, stronger tsunami flooding conditions were reproduced in the laboratory by using higher water levels, reaching the top of the mangrove canopy.

Stiff structure assumption

In order to compare the properties of a mangrove prototype and a mangrove model, three real-like models of a different root density (model group A with low density, model group B with medium density and model group C with high density) were constructed at a scale of 1:20 (Fig. 3). The trunk and the roots were modeled using a modeling clay, hardened in an oven. The relationship between the submerged root volume ratio and root submergence, plotted in Fig. 4a, agrees very well with the pattern determined by Mazda et al. (1997a). Geometry of these models is provided in Tables 1 and 2.

In the next step, three parameterized models for each real model were introduced, accounting for a varying frontal root area A_f (i.e. the area perpendicular to flow direction) with changing root submergence (see Fig. 3). The nature-like-shaped trunk and the roots were replaced in these models by steel and plastic cylinders of varying number, diameter and height (see Tables 1 and 2).

Based on results of experiments performed at a scale of 1:20 (Froude similitude law) under quasi-steady flow conditions, which aimed at a comparison of the properties of the real and the parameterized stiff mangrove models in terms of drag coefficient, reduction of flow velocity and hydraulic gradient, model A2 was selected as the best representation of the mangrove prototype. Detailed information on these experiments is provided in Husrin (2013).

Flexible structure assumption

The stiff mangrove model A2 was further modified into the flexible model by introducing a trunk and a canopy. Similarly to the stiff structure parameterization procedure, a real flexible mangrove model was constructed first to provide a reference for the parameterized flexible models (Fig. 4b and Table 3). The canopy and trunk in this model was made of plastic branches with leaves, resulting in a Leaf Area Index of 4.5. The parameterization of the mangrove prototype under flexible structure assumption was performed in two stages in order to determine the representative properties of the canopy and the trunk. In the first step, the five tree models were equipped with a stiff trunk, while the

canopy properties (density and frontal area) varied by controlling the volume of the fibrous material used (see Fig. 4b and Table 3). The models were examined under quasi-steady flow conditions in terms of current-induced forces (see Husrin 2013 for more details). Based on the comparison of the experimental data, canopy model M2FS was selected for the construction of the entirely flexible mangrove models (see Fig. 4b and Table 3). The trunk in the three flexible models was made of Polytetrafluoroethylene (PTFE), which is the only feasible material with elasticity (0.5×10^9 N/m^2 at model scale 1:25) fitting to the aforementioned range of the Young modulus for mangrove trunks. Density of this material (ca. 2000 kg/m^3) is however double as compared to mangrove trunk density (ca. 1000 kg/m^3). Comparative analysis of the deflection pattern of the flexible models (see Husrin 2013) indicated that model M2FF is the best representation on the mangrove prototype.

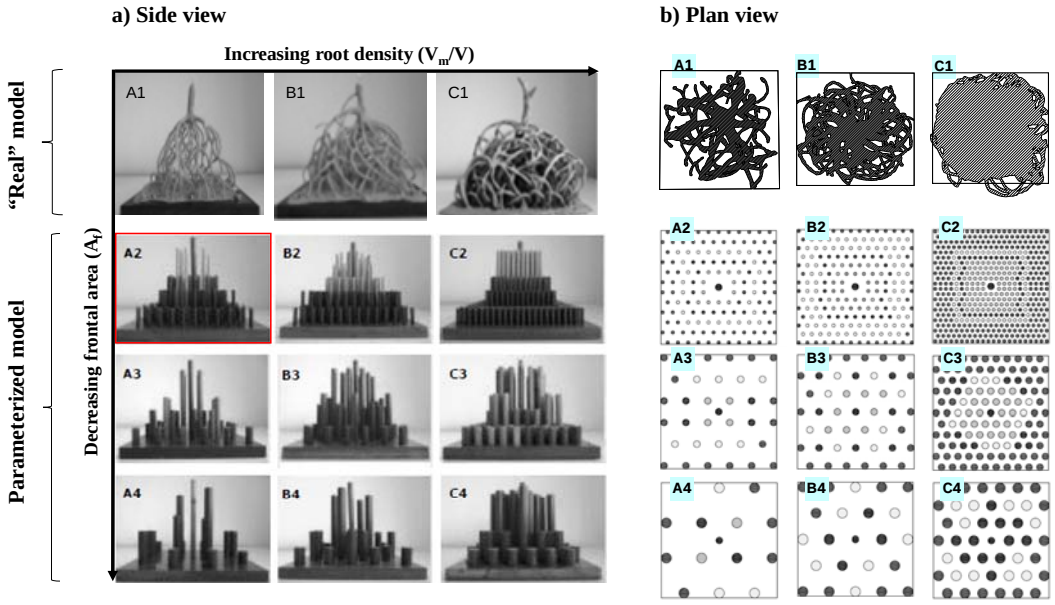

Figure 3. Developed stiff mangrove models: a) side view, b) plan view. The root model applied to the flexible mangrove models is marked in red frame.

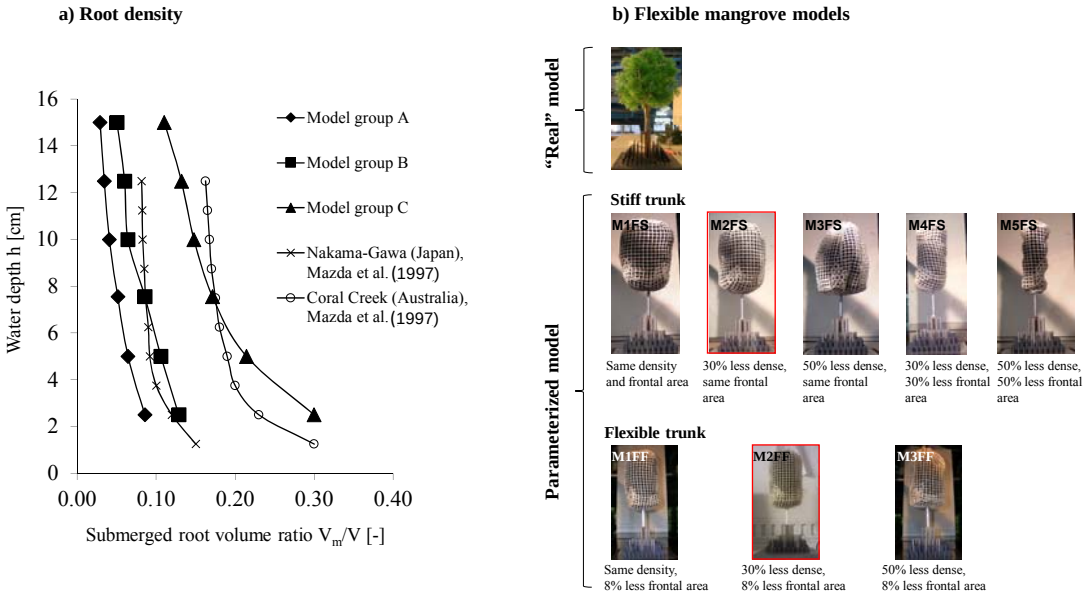

Figure 4. Relationship between mangrove root density and root submergence (a) and constructed flexible mangrove models (b). The selected flexible model is marked in red frame.

Table 1. Properties of stiff mangrove models at model scale of 1:20 (height and diameter in cm).

Structural part		Model group A				Model group B				Model group C			
		A1	A2	A3	A4	B1	B2	B3	B4	C1	C2	C3	C4
Trunk	No.	1	1	1	1	1	1	1	1	1	1	1	1
	Height	15	15	15	15	15	15	15	15	15	15	15	15
	Diameter	1	1	1	1	1	1	1	1	1	1	1	1
Root type I	No.	9	12	4	2	12	20	8	4	16	96	24	12
	Height	-	12.5	12.5	12.5	-	12.5	12.5	12.5	-	12.5	12.5	12.5
	Diameter	0.6	0.5	1.0	1.5	0.6	0.5	1.0	1.5	0.6	0.5	1.0	1.5
Root type II	No.	26	0	0	0	40	12	0	0	40	0	0	0
	Height	-	10	10	10	-	10	10	10	-	10	10	10
	Diameter	0.4	0.5	1.0	1.5	0.4	0.5	1.0	1.5	0.4	0.5	1.0	1.5
Root type III	No.	20	20	4	2	40	28	8	0	40	44	12	0
	Height	-	7.5	7.5	7.5	-	7.5	7.5	7.5	-	7.5	7.5	7.5
	Diameter	0.35	0.5	1.0	1.5	0.35	0.5	1.0	1.5	0.35	0.5	1.0	1.5
Root type IV	No.	25	28	8	4	63	80	8	8	150	52	12	12
	Height	-	5.0	5.0	5.0	-	5.0	5.0	5.0	-	5.0	5.0	5.0
	Diameter	0.3	0.5	1.0	1.5	0.3	0.5	1.0	1.5	0.3	0.5	1.0	1.5
Root type IV	No.	-	74	18	4	-	46	20	10	-	474	66	20
	Height	-	2.5	2.5	2.5	-	2.5	2.5	2.5	-	2.5	2.5	2.5
	Diameter	-	0.5	1.0	1.5	-	0.5	1.0	1.5	-	0.5	1.0	1.5

Table 2. Frontal area of stiff mangrove models for relative root submergence h/h_{mdl} = 0.05-0.15 at model scale of 1:20 (h_{mdl} denotes total mangrove model height).

A1: 30.6-61.8 cm^2	A2: 50.1-86.6 cm^2	A3: 47.5-75.0 cm^2	A4: 41.3-66.3 cm^2
B1: 34.7-70.1 cm^2	B2: 65.1-119.1 cm^2	B3: 47.5-125.0 cm^2	B4: 45.0-110.0 cm^2
C1: 56.9-115.1 cm^2	C2: 72.6-142.9 cm^2	C3: 74.3-148.2 cm^2	C4: 84.0-171.1 cm^2

Table 3. Characteristics of flexible mangrove models (model scale of 1:25).

Model	ReMS	M1FS	M2FS	M3FS	M4FS	M5FS	M1FF	M2FF	M3FF
Total submerged volume [cm^3]	165.20	174.20	116.16	87.10	116.16	87.10	174.20	116.16	87.10
Canopy width [m]	0.150	0.135	0.135	0.135	0.095	0.068	0.124	0.124	0.124
Canopy frontal area [m^2]	0.0291	0.0297	0.0297	0.0297	0.0208	0.0148	0.0273	0.0273	0.0273

EXPERIMENTAL SET-UP

Experimental facility

The laboratory investigation on solitary wave attenuation by the parameterized mangrove forest was conducted in a 2 m – wide wave flume at the Leichtweiss-Institute for Hydromechanics and Coastal Engineering at the Technical University of Braunschweig in Germany. The flume is approximately 90 m long and 1.25 m deep and is equipped with a piston type wave maker (see Fig. 5a). The model was scaled according to Froude similitude law, using a scale of 1:25.

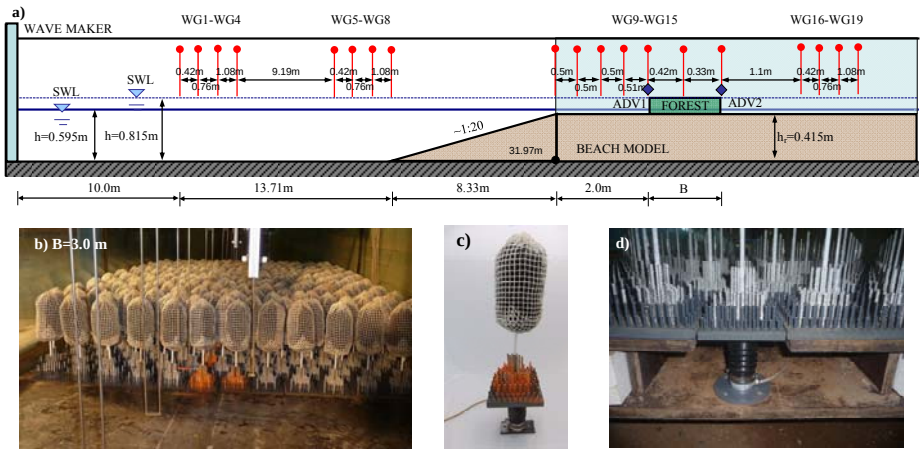

Figure 5. Experimental set-up: a) arrangement of measuring devices, b) forest model of width of *B*=3.0 m, c) force transducer connected to mangrove model, d) installation of force transducer in forest model.

Mangrove forest model and beach model

In order to investigate the conditions most favorable for wave attenuation, maximum possible forest density was considered in this test series, corresponding to ca. 44 trees/m^2. This density was achieved by arranging the tree models in shifted rows, consisting of 12 and 13 mangrove models (see Figs. 5b and 6). 62 and 250 mangrove tree models were used to construct forest model of width of B = 0.75 m and B = 3.0 m, respectively.

A proper modelling of a bathymetry/topography as well as applied wave force measurement technique (described in more details in the following section) required placement of the forest model on an elevated ground. A horizontal plywood platform, representing a beach model of height of ca. 0.41 m and a seaside slope of 1:20, was constructed for this purpose. The toe of the beach model was placed at a distance of ca. 23.7 m from the wave maker, while the front of the forest model was 33.97 m from the wave generator and 2.0 m behind the end of the beach slope, as shown in Fig. 5a.

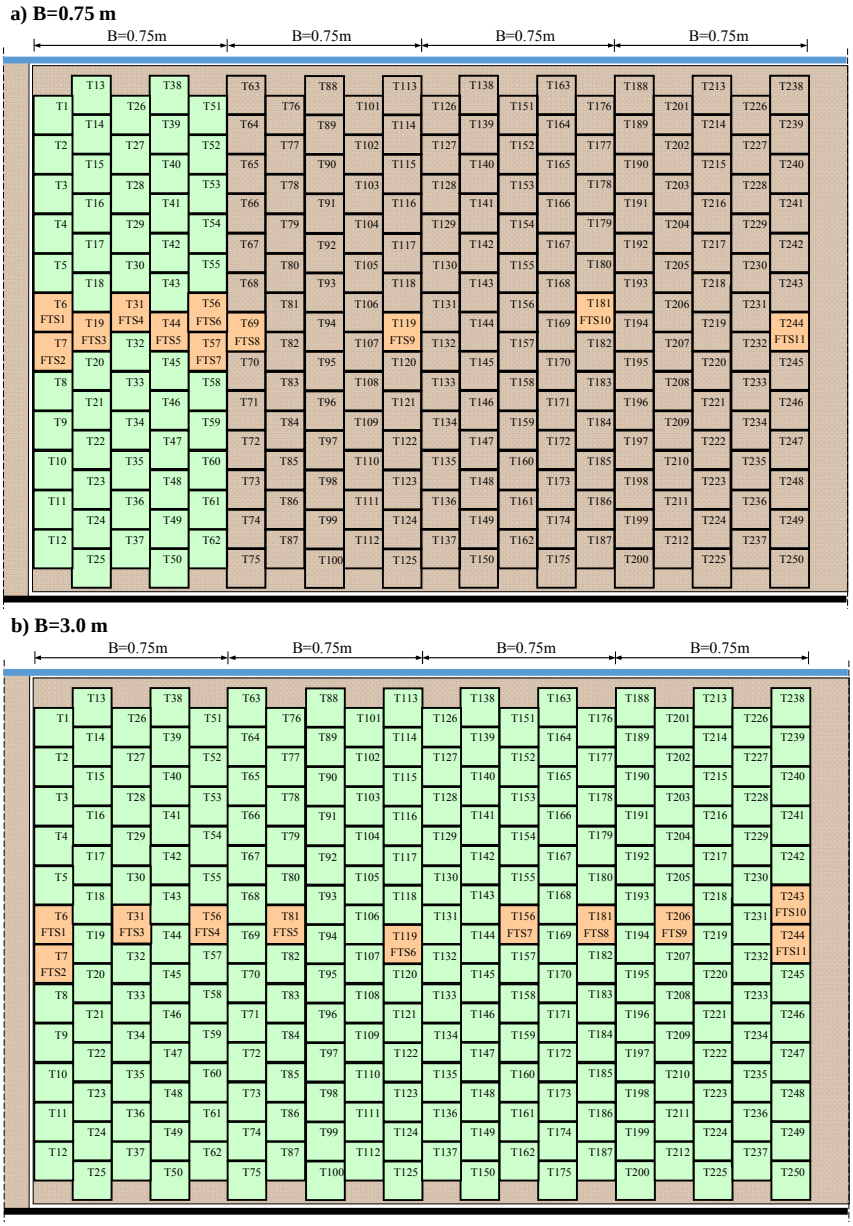

Figure 6. Arrangement of mangrove tree models (green squares marked as T1 - T250) and force transducers (orange squares marked as FT1 - FT11) in forest model of width of: a) 0.75 m, b) 3.0 m.

Measuring technique

The pattern of wave propagation in front of, in, and behind the mangrove forest model was recorded by means of 19 wire-type wave gauges (WG), which arrangement is presented in Fig. 5a. Three wave gauges were placed within the forest model: wave gauge WG13 at the front, WG14 in the middle and WG15 at the rear tree row.

In addition to the wave profile analysis, the pattern of wave forces induced on single tree models was examined by means of force transducers (FT), developed at the LWI for the purposes of this investigation (Figs. 5c and d). The force transducers are capable of measuring positive and negative wave forces up to 60 N, exerted in the direction of wave propagation. In each forest model configuration, 11 force transducers were employed within the forest, and in case of the shorter forest model (B = 0.75 m), also behind the forest as depicted in Fig. 6.

Two Acoustic-Doppler velocimeters (ADV), installed at the beginning and at the end of the forest model, measured horizontal flow velocity in the direction of wave propagation (see Fig. 5a).

Experimental programme

For each of the considered configurations of the mangrove forest model (i.e. forest width of 0.75 m and 3.0 m), varying water depth conditions and solitary wave height were examined, what resulted in a total number of 50 tests. In order to investigate the influence of the submergence of the mangrove tree model on solitary wave attenuation, total water depth in front of the beach model h was varied from 0.595 m to 0.815 m (with an increment of 0.055 m), which corresponded to the tree model submergence range of d_r = 0.18 - 0.40 m. As shown in Fig. 7, the tree submergence covered the entire height of tree canopy, with the lowest submergence reaching the canopy bottom and the highest one reaching canopy top. For each water level, solitary waves of five different nominal incident heights ($H_{i,nom}$ = 0.04, 0.08, 0.012, 0.016 and 0.20 m) were generated.

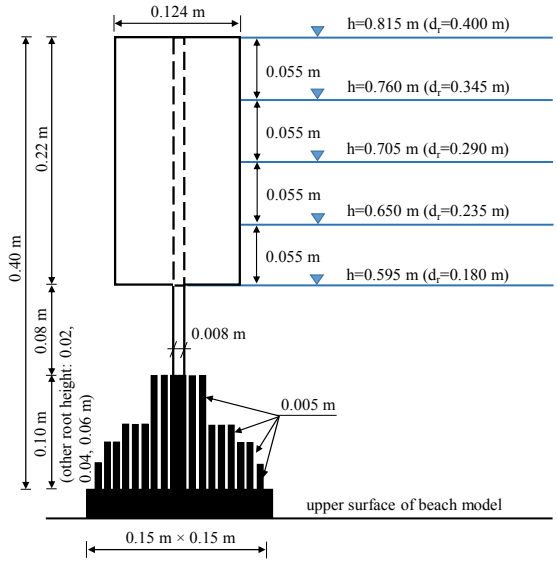

Figure 7. Examined water depth conditions in respect to the geometry of flexible mangrove model.

ANALYSIS OF EXPERIMENTAL RESULTS

Classification of wave evolution modes

Due to the fact that two sources of wave energy attenuation were observed in the conducted tests, namely the wave-forest interaction and wave breaking process, introduction of wave evolution modes into the data analysis was very crucial for the proper assessment of the forest damping performance. In case of tests with nonbreaking solitary waves, which dominated in the performed test series, the reduction of wave energy was solely due to wave propagation in the forest model. In contrast, in the experiments under broken wave conditions, both the forest model and the bathymetry/topography contributed to wave attenuation. The classification of the wave evolution modes was based both on the generation of wave breaking and the location of the breaking point in respect to the geometry of the beach-forest model. The following wave evolution modes (EM) were distinguished:

1. **Nonbreaking solitary waves disintegrating into solitons:**

- Nonbreaking waves (EM1): a solitary wave train, consisting of waves of decreasing height (solitons), was generated as a result of the wave fission process due to the change of the water depth over the beach model (see Fig. 8a).

2. **Breaking solitary waves disintegrating into solitons:**

- Waves breaking between the end of the beach slope and the beginning of the forest model (region 2) and disintegrating into solitons (EM3), as illustrated in Fig. 8b.
- Waves breaking in the forest model (region 3) and disintegrating into solitons (EM4), shown in Fig. 8c.
- Waves breaking behind the forest model (in region 4) and disintegrating into solitons (EM5), depicted in Fig. 8d.

Evolution mode EM2, in which wave broke over the beach slope (in region 1), was not observed in the performed test series. As shown in Fig. 9, the wave evolution modes were governed predominantly by the incident solitary wave height and the water depth, and partially by the width of the forest model (to distinguish between wave breaking induced in and behind the forest model).

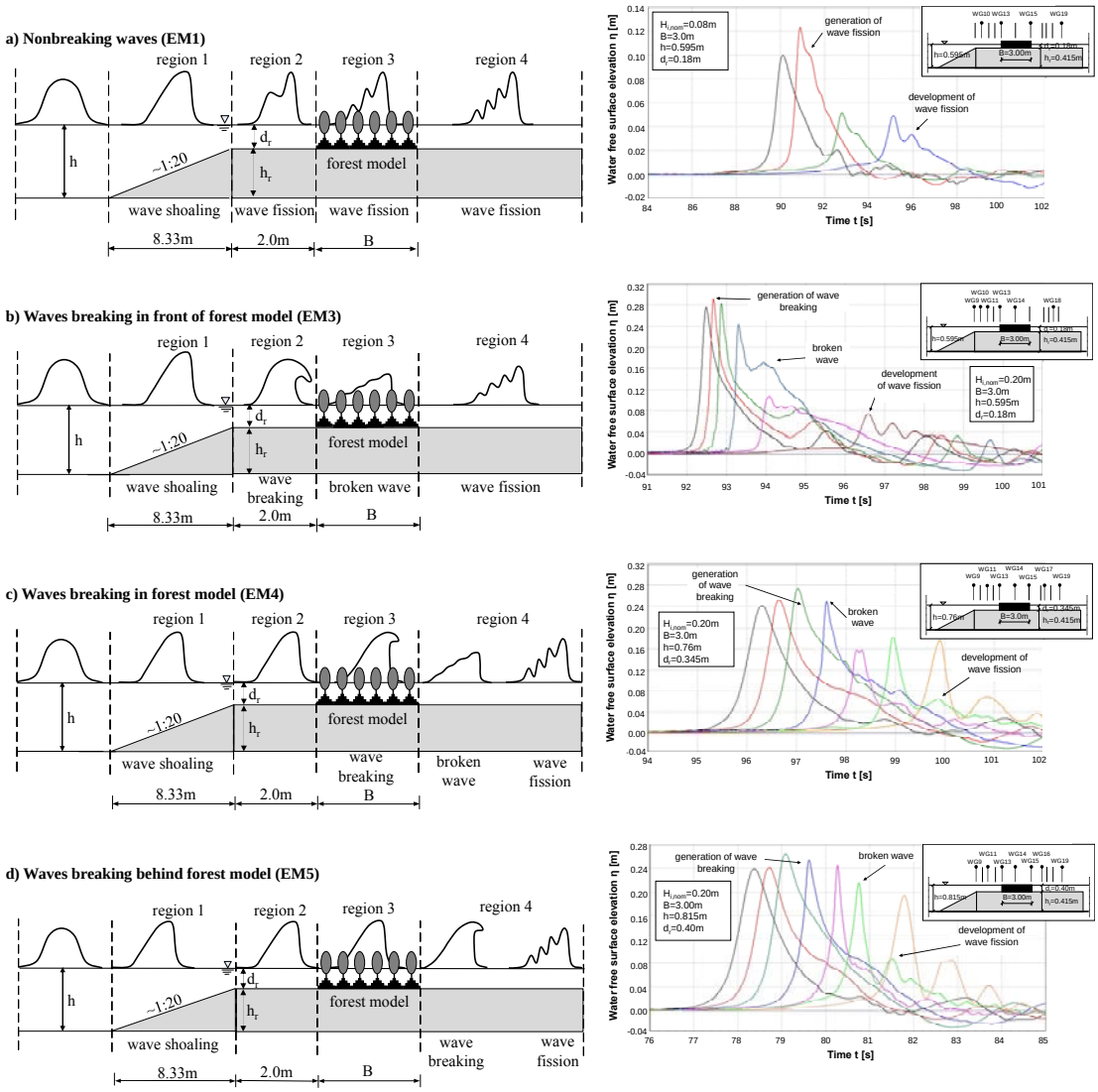

Figure 8. Classification of wave evolution modes.

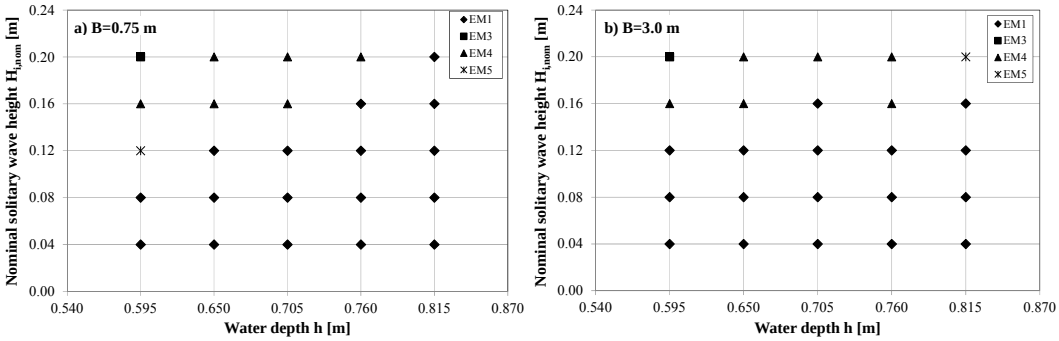

Figure 9. Observed wave evolution modes as a function of water depth conditions and solitary wave height in case of forest width of: a) *B* = 0.75 m, b) *B* = 3.0 m.

Evolution of wave height

Effectiveness of the forest model in wave attenuation was analyzed first in terms of solitary wave height reduction, which was governed forest width, water level and incident wave height. For this purpose, maximum solitary wave height was determined for each performed experiment. Exemplary results of this analysis, plotted in Fig. 10 for both forest model configurations and extreme water level conditions examined, clearly indicate four regions of different wave behavior. Solitary wave height remained constant over the horizontal part of the flume and increased as a result of shoaling process over the slope of the beach model. Depending on the evolution mode, the wave height decreased either in front of the forest model due to wave breaking process (wave evolution mode EM3), or in the forest model (EM1 and EM4), where particularly significant wave height reduction was observed for the wider forest model. The wave height in front of the forest model yielded: ca. 0.05 m for $H_{i,nom}$ = 0.04 m, 0.1 m for $H_{i,nom}$ = 0.08 m, 0.15 - 0.20 m for $H_{i,nom}$ = 0.12 m, 0.20 - 0.25 m for $H_{i,nom}$ = 0.16 m and 0.23 - 0.27 m for $H_{i,nom}$ = 0.20 m for all examined water depths. These wave heights were attenuated as follows at the end of the forest model of width of 0.75 m: ca. 0.02 - 0.04 m for $H_{i,nom}$ = 0.04 m, 0.07 m for $H_{i,nom}$ = 0.08 m, 0.11 m for $H_{i,nom}$ = 0.12 m, 0.12 - 0.16 m for $H_{i,nom}$ = 0.16 m and 0.14 - 0.20 m for $H_{i,nom}$ = 0.20 m for all examined water depths. As a result of a longer propagation distance in case of the forest model of width of 3.0 m, further wave height reduction was observed at the rear tree row: ca. 0.03 m for $H_{i,nom}$ = 0.04 m, 0.05 m for $H_{i,nom}$ = 0.08 m, 0.06 - 0.10 m for $H_{i,nom}$ = 0.12 m, 0.07 - 0.16 m for $H_{i,nom}$ = 0.16 m and 0.08 - 0.24 m for $H_{i,nom}$ = 0.20 m for all examined water depths.

The pattern of solitary wave height behind the forest model was generally more irregular for higher water levels and forest model of B = 0.75 m due to the more intensive process of solitary wave fission and triggering of wave breaking behind the forest (EM5).

Evolution of wave forces induced on single mangrove models

Pattern of maximum wave forces exerted on the single mangrove models was analyzed in a similar way to the envelope of the maximum solitary wave height. Fig. 11 presents exemplarily the development of the forces in the forest for representative experiments, in which point 0.0 m on the horizontal axis represents the beginning of the forest model. The magnitude of the wave forces was governed by the water depth and wave height conditions and the resulting evolution mode – the forces decreased with the increasing submergence depth of the tree models and on the other hand they became larger for greater wave heights, e.g. ca. 1 N for $H_{i,nom}$ = 0.04 m, 5 - 6.5 N for $H_{i,nom}$ = 0.08 m, 7 - 15 N for $H_{i,nom}$ = 0.12 m, 10 - 24 N for $H_{i,nom}$ = 0.16 m and 13 - 27 N for $H_{i,nom}$ = 0.20 m for all examined water depths.

The highest forces were exerted at the frontal tree row at the direct impact of the wave. A general trend of the decrease of the wave forces with wave propagation in the forest model was observed (see FT1 - 7 for B = 0.75 m and FT1 - 11 for B = 3.0 m in Fig. 11). A smaller force reduction was attributed to the narrow forest model due to the shorter wave propagation distance and thus weaker interaction with the tree models. The forces recorded at the end of this forest model corresponded well to that measured by force transducers FT4 in forest of width of 3.0 m and yielded: ca. 0.7 - 1 N for $H_{i,nom}$ = 0.04 m, 3 - 4 N for $H_{i,nom}$ = 0.08 m, 6 - 9 N for $H_{i,nom}$ = 0.12 m, 9 - 15 N for $H_{i,nom}$ = 0.16 m and 10 - 15 N for $H_{i,nom}$ = 0.20 m for all examined water depths. Further reduction of the forces (between FT4 and FT10/11) was observed within the wide forest model.

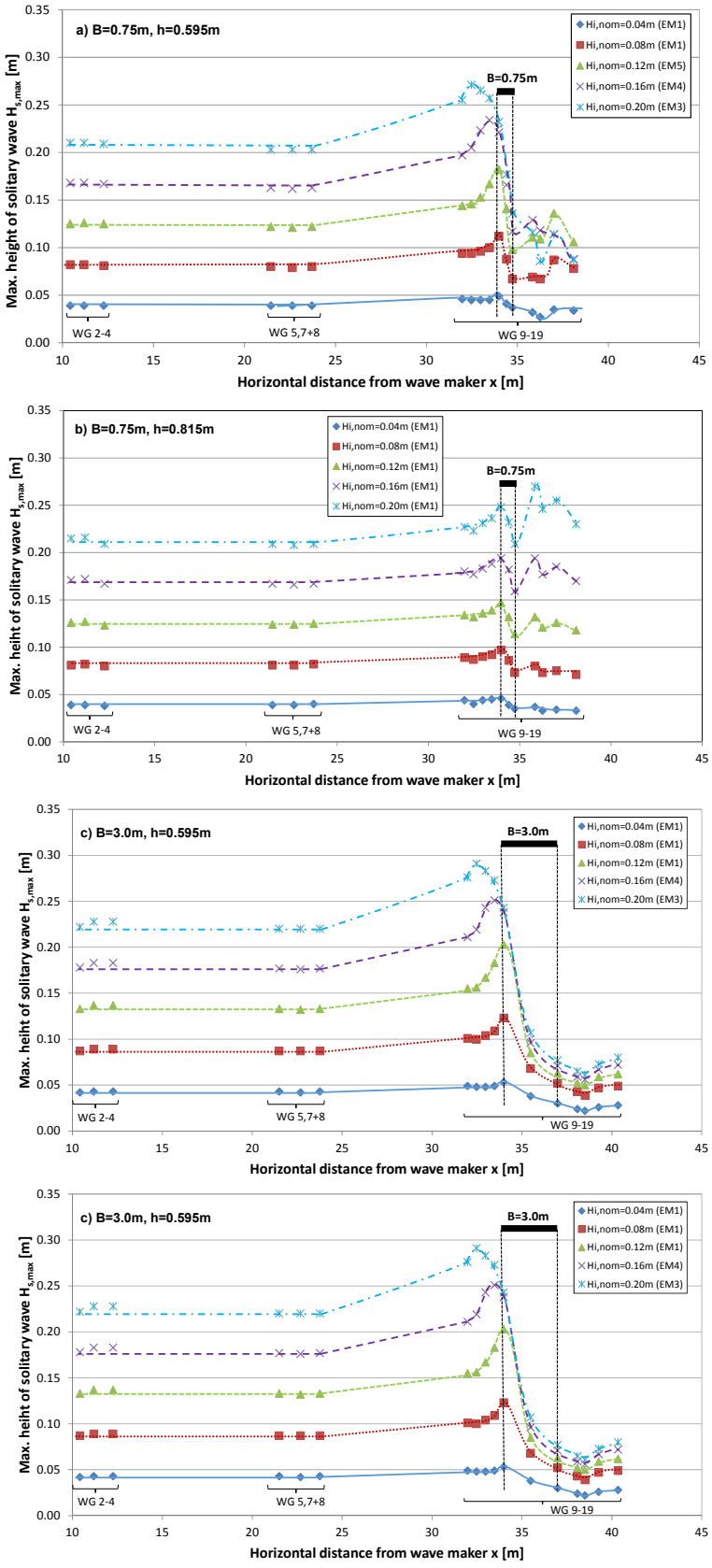

Figure 10. Envelopes of maximum solitary wave height for: a) *B* = 0.75 m and *h* = 0.595 m, b) *B* = 0.75 m and *h* = 0.815 m, c) *B* = 3.0 m and *h* = 0.595 m, d) *B* = 3.0 m and *h* = 0.815 m.

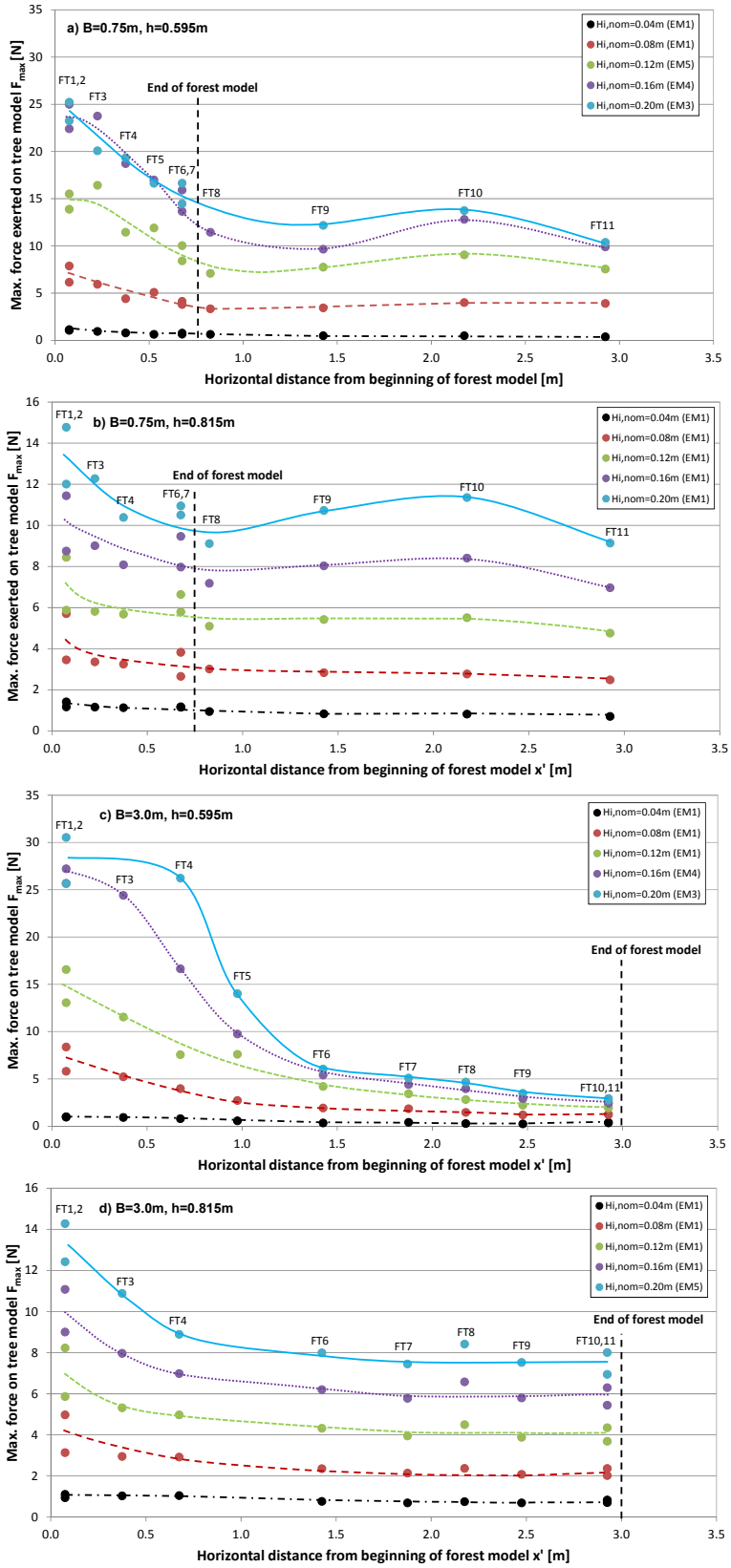

Figure 11. Envelopes of maximum wave forces exerted on single mangrove models for: a) *B* = 0.75 m and *h* = 0.595 m, b) *B* = 0.75 m and *h* = 0.815 m, c) *B* = 3.0 m and *h* = 0.595 m, d) *B* = 3.0 m and *h* = 0.815 m.

The range of the wave forces at the end of this forest model was as follows: ca. 0.4 - 0.8 N for $H_{i,nom}$ = 0.04 m, 1.2 - 2.2 N for $H_{i,nom}$ = 0.08 m, 2 - 4 N for $H_{i,nom}$ = 0.12 m, 2.4 - 6 N for $H_{i,nom}$ = 0.16 m and 2.8 - 7.5 N for $H_{i,nom}$ = 0.20 m for all examined water depths. The additional contribution of the breaking process to wave attenuation in the forest can be clearly seen in Figs. 11a and c, what resulted in a greater reduction of the wave forces as compared to the nonbreaking waves.

In case of the narrow forest model, the data measured by the force transducers placed behind the forest model (FT8 - 11) indicate a slight increase and then decrease of the forces to the value behind the forest model, particularly for larger wave heights. Due to the limited number of the constructed force transducers, analysis of this force pattern behind forest model of B = 3.0 m was not possible and requires further investigation.

Wave transmission

Due to the disintegration of the incident solitary wave into a soliton train, wave transmission coefficient was calculated as a function of wave energy as postulated by Liu and Cheng (2001). Wave energy was considered as a sum of kinetic and potential wave energy (Longuet-Higgins and Fenton 1974):

$$E_{tot} = E_k + E_p, \tag{1}$$

determined at wave gauge WG13 as total energy of incident wave and at WG15 as total energy of transmitted wave. The energy components are expressed as follows:

$$E_k = 0.5\rho \int_{-\infty}^{\infty} \int_{-h}^{\eta} u^2 dz dx, \tag{2}$$

$$E_p = 0.5\rho \cdot g \int_{-\infty}^{\infty} \eta^2 dx. \tag{3}$$

Approach by Al-Banaa und Liu (2007) was used to transform the energy components from spatial into temporal domain:

$$E_k = 0.5\rho \cdot c \int_{t_1}^{t_2} \int_{-h}^{\eta} u^2 \, dz dt, \tag{4}$$

$$E_p = 0.5\rho \cdot g \cdot c \int_{t_1}^{t_2} \eta^2 dt, \tag{5}$$

in which $dx = c \cdot dt$. The horizontal particle velocity can be defined after Munk (1949) as:

$$u = c \frac{\eta}{h + \eta}, \tag{6}$$

with solitary wave speed calculated as:

$$c = \sqrt{g(h + H)}. \tag{7}$$

In Eqs. 1-7, c denotes the wave celerity [m/s], E_k the kinetic wave energy [J/m], E_p the potential wave energy [J/m], g the gravitational acceleration [m/s^2], h the water depth [m], H the wave height [m], u the horizontal particle velocity [m/s] and η the water free surface elevation [m].

Figure 12 shows the relationship between computed wave transmission coefficient K_t and relative forest width B/L with corresponding wave evolution modes. Two very clear data clouds can be distinguished in this graph: one for forest width of B = 0.75 m with the transmission coefficient ranging from ca. 0.48 to 0.78 and another for forest width of B = 3.0 m with K_t = 0.29 - 0.56. The lowest wave transmission was attributed to waves breaking in front of and in the forest model (EM3 and EM4, respectively) due to the combined wave energy dissipation through the wave-tree model

interaction and the turbulence at breaking. Nonbreaking waves (EM1) were dominant in the performed test series, resulting in much higher transmission coefficient as compared to the broken waves. A better performance of the forest model can be also observed for smaller water depths, particularly when comparing the data for a constant wave height.

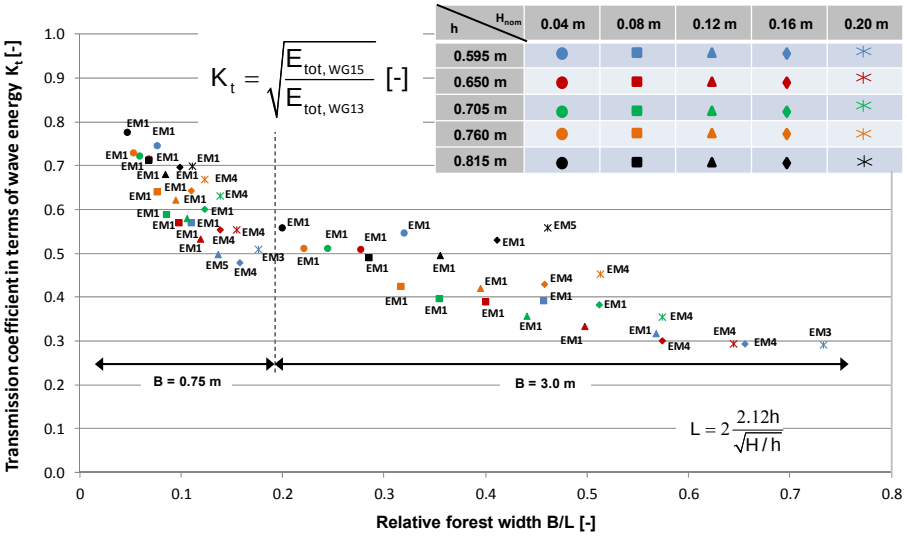

Figure 12. Wave transmission coefficient as a function of relative forest width.

CONCLUSIONS

Consideration of the most important physical properties of the selected mangrove species as well their dependency on the tree age makes the parameterization approach presented in this paper more reliable than those proposed in the previous studies. Although it was developed for a specific tree species, the assumptions made and the systematic parameterization procedure itself can be applied to other types of coastal vegetation. However, there are two shortcomings of the parameterization procedure to be mentioned: firstly, experimental modelling of a tree failure (e.g. trunk breakage or uprooting) under wave impact is not possible and secondly, the trunk model, despite same elasticity as mangrove wood, has density that is double density of the prototype.

The idealized forest conditions assumed in these experiments, namely the maximum forest density, healthy mangrove trees of idealized resistance to wave attack, result in overestimation of the attenuation performance of the forest model. As indicated by the results, wave energy reduction by 70% was attributed to the widest forest of B = 3.0 m (75 m in prototype) in case of the weakest flow depth conditions examined. In case of larger flow depths, reaching the top of the canopy, wave transmission is reduced to ca. 40 - 50%. Despite such a large forest width, relatively poor performance of the forest model was observed, which is, in fact, even poorer when considering the horizontal scale of a real tsunami and laboratory limitations in generation of long waves. Moreover, execution of such large vegetation zones at the coast would be very difficult in many regions due to the limited availability of the land. The effectiveness of the narrower forest model of B = 0.75 m (18.75 m in prototype) is too low (between 20 and 50%) in order to consider the mangrove forest as a defense barrier against tsunami. Despite the low performance in attenuation of extreme tsunami, planning and maintenance of coastal green belts is highly recommended due to the coast stabilization functions and protection from flooding, mentioned before in the introductory part of this paper, as well as due to the life-saving role and debris-stoppage reported from the recent tsunami events.

ACKNOWLEDGMENTS

The TAPFOR project was performed in the framework of the project "Tracing Tsunami impacts on- and offshore in the Andaman Sea Region (TRIAS)", funded by the Deutsche Forschungsgemeinschaft (DFG) and the Office of the Research Council of Thailand (NRCT) and partly by the DFG within the Graduate College of TU Braunschweig "Risk Management of Natural and Civilization Hazards on Buildings and Infrastructure" (GRK 802).

REFERENCES

Al-Banaa, K., and P.L.-F. Liu. 2007. Numerical study on the hydraulic performance of submerged porous breakwater under solitary wave attack, *Journal of Coastal Research*, Special Issue 50, 201-205.

Badola, R., and S.A. Hussain. 2005. Valuing ecosystem functions: an empirical study on the storm protection function of Bhitarkanika mangrove ecosystem, India, *Environmental Consecration*, 32(1), 85-92.

Clough, B.F., D.T. Tan, D.X. Phuong, and D.C. Buu. 2000. Canopy leaf area index and litter fall in stands of the mangrove Rhizophora apiculata of different age in the Mekong Delta, Vietnam, *Aquatic Botany*, 66(4), 311-320.

EJF. 2006. *Mangroves: nature`s defence against tsunamis - a report on the impact of mangrove loss and shrimp farm development on coastal defences*, Environmental Justice Foundation, London, UK.

Green, E., and C. Clark. 2000. *Assessing mangrove Leaf Area Index and canopy closure*, Remote Sensing Handbook for Tropical Coastal Management, J. Edwards (Ed.), UNESCO-CSI, http://www.unesco.org/csi/pub/source/rs.htm.

Harada, K., and F. Imamura. 2000. Experimental study on the resistance by mangrove under the unsteady flow, *Proceedings of the 1st Congress of the Asian and Pacific Coastal Engineering*, Dalian, 975-984.

Harada, K., and Y. Kawata. 2005. Study on tsunami reduction effect of coastal forests due to forest growth, *Annuals of Disaster Prevention Research Institute*, 48C, Tokyo University, Japan, 161-165.

Hawa, S. 2005. *The use of bakau as a piling material in Malaysia*, Bachelor thesis, Universiti Teknologi Malaysia, 166pp.

Husrin, S. 2013. *Modeling of tsunami and storm wave attenuation by coastal forests*, Doctoral Thesis, TU Braunschweig, Germany.

Istiyanto, D.C., K.S. Utomo, and Suranto. 2003. Pengaruh Rumpun Bakau Terhadap Perambatan Tsunami di Pantai (The effect of mangrove forest to the attenuation of tsunami in coastal area), *Proceedings of Seminar Mengurangi Dampak Tsunami: Kemungkinan Penerapan Hasil Riset, BPPT - JICA, 11 March 2003, Yogyakarta* (in Indonesian).

Kathiresan, K., and N. Rajendran. 2005. Coastal mangrove forests mitigated tsunami, *Estuarine, Coastal and Shelf Science*, 65(3), 601-606.

Kongko, W. 2004. Study on tsunami energy dissipation in mangrove forest, *Master Thesis*, Iwate University, Japan.

Latief, H., and S. Hadi. 2006. The role of forest and trees in protecting coastal areas against tsunami, *Proceedings of the Regional Technical Workshop "Coastal protection in the aftermath of the Indian Ocean tsunami: what role for forests and trees?"*, Khao Lak, Thailand.

Liu, P.L.-F., and Y. Cheng. 2001. A numerical study of the evolution of a solitary wave over a shelf, *Physics of Fluids*, 40(3), 229-240.

Longuet-Higgins, M.S., and J.D. Fenton. 1974. On the mass, momentum, energy and circulation of a solitary wave, *Proceedings Royal Society London A*, 337, 1-13.

Massel, S.R., K. Furukawa, and R.M. Brinkman. 1999. Surface waves propagation in mangrove forests, *Fluid Dynamics Research*, 24, 219-249.

Mazda, Y., E. Wolanski, B. King, A. Sase, D. Ohtsuka, and M. Magi. 1997a. Drag force due to vegetation in mangrove swamps, *Mangroves and Salt Marshes*, 1, 193-199.

Mazda, Y., M. Magi, M. Kogo, and P.N. Hong. 1997b. Mangroves as a coastal protection from waves in the Tong King delta, Vietnam, *Mangroves and Salt Marshes*, 1, 127-135.

Munk, W. 1949. The solitary wave theory and its application to surf problems, *Annals of the New York Academy of Sciences*, 51, 376-424.

Shuto, N. 1987. The effectiveness and limit of tsunami control forests, *Coastal Engineering in Japan*, 30, 143-153.

Strusińska-Correia, A., S. Husrin, and H. Oumeraci. 2013. Tsunami damping by mangrove forest: a laboratory study using parameterized trees, *Journal of Natural Hazards and Earth System Sciences*, 13, 483-503.

Vallam, S., M. Kantharaj, and N. Lakshmanan. 2011. *Resistance of flexible emergent vegetation and their effects on the forces and runup due to waves*, In: The Tsunami Threat - Research and Technology, www.intechopen.com, 129-160.

Wolanski, E. 2007. Protective functions of coastal forests and trees against natural hazards. In: *Coastal Protection in the Aftermath of the Indian Ocean Tsunami. What Role for Forests and Trees?* FAO, Bangkok, 157-179.

Yanagisawa, H., S. Koshimura, K. Goto, T. Miyagi, F. Imamura, A. Ruangrassamee, and C. Tanavud. 2009. The reduction effects of mangrove forest on a tsunami based on field surveys at Pakarang Cape, Thailand and numerical analysis, *Estuarine, Coastal and Shelf Science*, 81, 27-37.